University of Nebraska - Lincoln

DigitalCommons@University of Nebraska - Lincoln

USGS Staff -- Published Research   US Geological Survey

2011

The rise and fall of Lake Bonneville between 45 and 10.5 ka

L.V. Benson
U.S. Geological Survey, great.basin666@gmail.com

S.P. Lund
University of Southern California, slund@usc.edu

J.P. Smoot
U.S. Geological Survey, jpsmoot@usg.gov

D.E. Rhode
Desert Research Institute, dave@dri.edu

R.J. Spencer
University of Calgary, spencer@ucalgary.ca

See next page for additional authors

Authors

L.V. Benson, S.P. Lund, J.P. Smoot, D.E. Rhode, R.J. Spencer, K.L. Verosub, L.A. Louderback, C.A. Johnson, R.O. Rye, and R.M. Negrini

The rise and fall of Lake Bonneville between 45 and 10.5 ka

L.V. Benson [a,*], S.P. Lund [b], J.P. Smoot [c], D.E. Rhode [d], R.J. Spencer [e], K.L. Verosub [f], L.A. Louderback [g], C.A. Johnson [h], R.O. Rye [h], R.M. Negrini [i]

[a] U.S. Geological Survey, 3215 Marine Street, Boulder, CO 80303, USA
[b] Department of Earth Sciences, University of Southern California, Los Angeles, CA 90089, USA
[c] U.S. Geological Survey, MS 955, Reston, VA 22092, USA
[d] Earth and Ecosystem Sciences, Desert Research Institute, 2215 Raggio Parkway, Reno, NV 89512, USA
[e] Department of Geology and Geophysics, University of Calgary, Alberta T2N 1N4, Canada
[f] Department of Geology, University of California, Davis, CA 95616, USA
[g] Department of Anthropology, University of Washington, Box 353100, Seattle, WA 98195-3100, USA
[h] U.S. Geological Survey, MS 963, Denver Federal Center, Lakewood, CO 80225, USA
[i] Department of Geology, California State University, Bakersfield, CA 93311-1022, USA

ARTICLE INFO

Article history:
Available online 23 December 2010

ABSTRACT

A sediment core taken from the western edge of the Bonneville Basin has provided high-resolution proxy records of relative lake-size change for the period 45.1−10.5 calendar ka (hereafter ka). Age control was provided by a paleomagnetic secular variation (PSV)-based age model for Blue Lake core BL04-4. Continuous records of $\delta^{18}O$ and total inorganic carbon (TIC) generally match an earlier lake-level envelope based on outcrops and geomorphic features, but with differences in the timing of some hydrologic events/states. The Stansbury Oscillation was found to consist of two oscillations centered on 25 and 24 ka. Lake Bonneville appears to have reached its geomorphic highstand and began spilling at 18.5 ka. The fall from the highstand to the Provo level occurred at 17.0 ka and the lake intermittently overflowed at the Provo level until 15.2 ka, at which time the lake fell again, bottoming out at ∼14.7 ka. The lake also fell briefly below the Provo level at ∼15.9 ka. Carbonate and $\delta^{18}O$ data indicate that between 14.7 and 13.1 ka the lake slowly rose to the Gilbert shoreline and remained at about that elevation until 11.6 ka, when it fell again. Chemical and sedimentological data indicate that a marsh formed in the Blue Lake area at 10.5 ka.

Relatively dry periods in the BL04-4 records are associated with Heinrich events H1−H4, suggesting that either the warming that closely followed a Heinrich event increased the evaporation rate in the Bonneville Basin and (or) that the core of the polar jet stream (PJS) shifted north of the Bonneville Basin in response to massive losses of ice from the Laurentide Ice Sheet (LIS) during the Heinrich event. The second Stansbury Oscillation occurred during Heinrich event H2, and the Gilbert wet event occurred during the Younger Dryas cold interval. Several relatively wet events in BL04-4 occur during Dansgaard-Oeschger (DO) warm events.

The growth of the Bear River glacier between 32 and 17 ka paralleled changes in the values of proxy indicators of Bonneville Basin wetness and terminal moraines on the western side of the Wasatch Mountains have ages ranging from 16.9 to 15.2 ka. This suggests a near synchroneity of change in the hydrologic and cryologic balances occurring in the Bonneville drainage system and that glacial extent was linked to lake size.

1. Introduction

Approximately 15,000 years ago, lakes in the Great Basin of the western United States achieved their maximum late Pleistocene extents. Two of those lake systems stand out in terms of surface area: Lake Lahontan with a surface area of 22,300 km², and Lake Bonneville with a surface area of 51,300 km² (Fig. 1). These gigantic fresh-

* Corresponding author.
 E-mail addresses: lbenson@usgs.gov (L.V. Benson), slund@usc.edu (S.P. Lund), jpsmoot@usg.gov (J.P. Smoot), dave@dri.edu (D.E. Rhode), spencer@ucalgary.ca (R.J. Spencer), klverosub@ucdavis.edu (K.L. Verosub), Lisbeth.louderback@gmail.com (L.A. Louderback), cjohnso@usgs.gov (C.A. Johnson), rnegrini@csub.edu (R.M. Negrini).
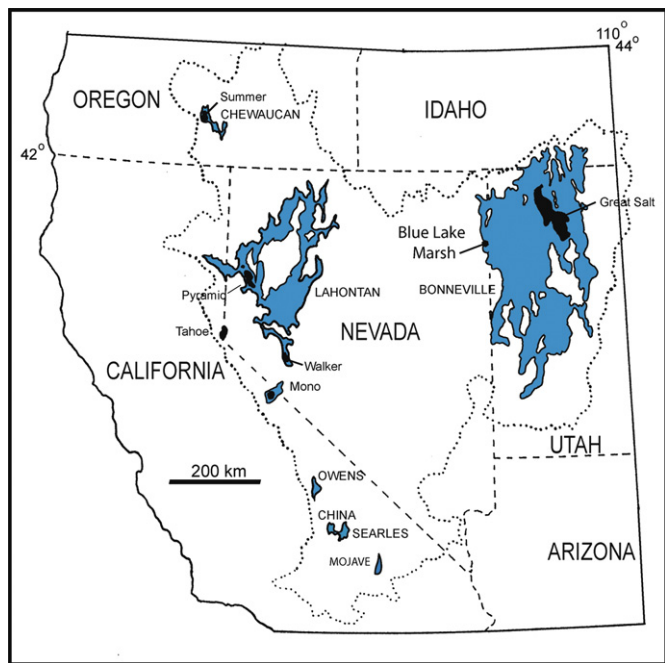
Fig. 1. Great Basin lakes about 15,000 years ago. The outline of the Great Basin is enclosed by a dashed line. The Blue Lake Marsh core sites are located on the western edge of Lake Bonneville near the Nevada–Utah border.

water bodies, which had surface areas approximately 10 times their reconstructed mean-historical values, have been the subject of intensive scientific research since Russell's seminal study of Lake Lahontan (Russell, 1885) and Gilbert's seminal study of Lake Bonneville (Gilbert, 1890). Three main questions have occupied the minds of present-day paleoclimatologists working in these two basins: (1) what caused the lakes to grow so large, (2) what was the record of lake-level change in each basin during the last glacial period, and (3) were lake-size changes linked to abrupt changes in the climate of the North Atlantic signaled by Dansgaard-Oeschger and Heinrich events (see, e.g., Bond et al., 1993; Dansgaard et al., 1993).

In terms of the process that led to the formation of the pluvial lakes, Antevs (1948) was the first to suggest that the size of the Laurentide Ice Sheet (LIS), combined with the presence of a permanent high-pressure area over it, caused storm tracks associated with the polar jet stream (PJS) to be pushed south of their present-day average path over the northern Great Basin. Atmospheric simulations of the global climate during the last ice age gave support to Antev's hypothesis (e.g., Kutzbach and Guetter, 1986), and a further test of this hypothesis was conducted by Hostetler and Benson (1990) when they imposed a PJS climatology on the Lahontan Basin. They used a physically based lake model to simulate changes in lake temperature and evaporation that occurred in response to changes in the lake-surface energy balance and in a small set of atmospheric parameters. It was found that a mean-annual cloud cover of 69% (associated with the presence of the PJS) was sufficient to decrease lake evaporation by 42%. This combined with a substantial (3.8 times the mean-historical value) increase in surface-water input to the basin was sufficient to produce the highstand of Lake Lahontan.

Benson and Thompson (1987, p. 255) suggested that when the PJS was forced south over the Lahontan and Bonneville basins, it created the thermal instability necessary to trigger lake-effect precipitation, leading to increases in lake size and glacier extent. Somewhat later, Hostetler et al. (1994), using a high-resolution, regional climate model, nested within a general circulation model, showed that lake-

generated precipitation indeed was a substantial component of the hydrologic budget of Lake Bonneville 18,000 years ago.

The creation of records of change in the size of lakes in the Lahontan and Bonneville basins are of two types: outcrop-based studies from which were created discontinuous envelopes of lake-level change, and core-based studies which allow continuous or nearly continuous proxy records of relative changes in lake level. The Bonneville Basin has provided detailed 36,000-year, outcrop-based records of change in the hydrologic balance of the eastern Great Basin (see e.g., Currey and Oviatt, 1985; Oviatt et al., 1992; Godsey et al., 2005). Oviatt (1997) produced isotopic, carbonate mineralogy, and TIC records from two short (<2 m) cores that penetrated subaerially exposed deep-water carbonates. Sediments at the two core sites range in age from ∼20–14.5 ka. To date, Spencer et al. (1984) have been the only researchers to produce a non-outcrop, core-based record of change in the size of Lake Bonneville for the past 30 ka. Age control for this study was extremely limited and age models for the various sediment cores were based on linear extrapolation between three samples: the Mazama and Carson Sink tephras and a piece of wood. Two of the above studies (Oviatt, 1997; Oviatt et al., 2005) attempted to link oscillations in the size of Lake Bonneville with North Atlantic Heinrich and Younger Dryas events.

This paper provides continuous and nearly continuous, core-based records of change in the hydrologic balance of Lake Bonneville for the period 45.1–10.5 ka. The isotopic and carbonate records have a 50-year temporal resolution; i.e., each sample integrates 50 years of record. In addition, PSV-based age models are employed for the hydrologic-balance proxy records created in this study. The PSV concept was first applied in a study of the Wilson Creek Formation at Mono Lake, California, by Benson et al. (1998). Since that study, one of the authors (Steve Lund) has created master PSV (magnetic inclination, declination, and intensity) records derived from Holocene (0–10 ka) PSV records in North American lakes and from late Pleistocene (10–70 ka) marine PSV records from the North Atlantic Ocean. The marine PSV records are plotted on a calendar time scale based on the GISP2 chronology. The tie to the GISP2 chronology was determined by matching $\delta^{18}O$ and TIC oscillations in marine cores, which reflect the presence of Dansgaard-Oeschger (DO) cycles and Heinrich events, to the GISP2 $\delta^{18}O$ record. This study matched the PSV records from the Bonneville cores to the master marine PSV chronology, allowing assignment of GISP2 dates to the cores, and hence permitting direct comparison of the timing of North Atlantic GISP2 Heinrich and DO events with past variations in the Lake Bonneville hydrologic balance.

2. Previous studies of Bonneville lake-level variations: 36–10 ka

The outcrop-based record of change in the size of Lake Bonneville (Oviatt et al., 1992) includes a rise in lake level beginning about 31.7 ± 0.7 ^{14}C ka (36.0 ± 0.8 ka) and an oscillation in lake level between 21.5 and 20.4 ^{14}C ka (25.8–24.3 ka) (the Stansbury Oscillation).[1]

Sack (1999) obtained nine ^{14}C dates on gastropod shells (7 dates) and wood (2 dates) from sub-Provo deposits on the Provo geomorphic platform. The calibrated ages range from 25.6 ± 0.3 to

---

[1] Calibrations of ^{14}C ages in this paper were done using CALIB 6.01 (Stuiver et al., 2005). When a ^{14}C date without a reported standard error is referenced, an error of ±100 years was assumed for the purposes of the calibration. All calibrated and cosmogenicbased ages are assumed to be calendar years and are denoted by ka; uncalibrated radiocarbon years are reported as ^{14}C ka. In this paper, ka can refer to either a time interval or a point in time.

21.1 ± 0.3 ka, suggesting that lake level was constrained by the early Provo platform during part of the Stansbury Oscillation. The oldest sub-Provo date is on wood and is considered reliable; however, thin-shelled gastropods can acquire small amounts of modern ^{14}C in the subaerial zone and may date too young. A piece of charcoal collected from the top of a pre-Bonneville highstand soil has been dated to 15.25 ± 0.16 ^{14}C ka (18.6 ± 0.1 ka) (Oviatt, 1991), which puts the timing of the highstand sometime after this date.

Godsey et al. (2005) obtained two identical ^{14}C dates (15.08 ± 0.09 ^{14}C ka, 18.2 ± 0.1 ka) on gastropod (Stagnicola) samples from gravelly sands located just below the Bonneville shoreline. Two other ^{14}C dates obtained by Godsey et al. (2005) on Stagnicola samples from Bonneville shoreline deposits indicate that the lake remained at its highstand level until at least 14.37 ± 0.24 ^{14}C ka (17.5 ± 0.3 ka). Thus, data obtained by Oviatt et al. (1992) and

Godsey et al. (2005) suggest that the Bonneville highstand occurred sometime between ~18.6 and ~17.5 ka (Fig. 2A).

During the latter part of its highstand, the lake overflowed and incised its threshold near the town of Zenda, lowering its overflow level until it reached a bedrock threshold at Red Rock Pass, at which time it occupied the Provo shoreline (Gilbert, 1890; Malde, 1968). Light (1996) obtained the earliest date recorded for a Provo shore deposit (14.29 ± 0.12 ^{14}C ka (17.4 ± 0.2 ka) on Stagnicola). The amount of time that the lake remained at or near the Provo level after the highstand is arguable. Oviatt et al. (1992) suggested that Provo shoreline formation ended at about 14 ^{14}C ka (17.0 ± 0.1 ka), whereas Godsey et al. (2005) argued for an extended occupation of the Provo shoreline, ending at about 12 ^{14}C ka (13.8 ± 0.1 ka) (Fig. 2A). Godsey et al. (2005) based their argument on 10 samples with ^{14}C dates <12.5 ka, having paleo-elevations of 1440 ± 10 m (the approximate paleo-elevation of the Provo shoreline). Nine of the samples were carbonates (ostracodes, gastropods, tufas) and one sample was composed of plant debris, having a date of 12.09 ± 0.30 ^{14}C ka (14.1 ± 0.5 ka). The latter sample was previously obtained by Bright (1966) from sediments in Swan Lake, located in the southern part of Lake Bonneville's outlet. Bright (1966) argued that this sample is from the base of lake sediments that were deposited after Lake Bonneville fell from the Provo level.

In essence, Oviatt et al. (1992) and Godsey et al. (2005) are in agreement with regard to Bonneville levels between 18.6 and 17.0 ka; i.e., Bonneville reached its highstand level at 18.6 ka; it fluctuated near that level until 17.5 ka, at which time it incised its threshold, reaching the Red Rock Pass level at 17.4 ka. Oviatt et al. (1992) believed that the lake stayed at or near that level until 17.0 ka whereupon it fell to near-historical levels by 13.8 ka. On the other hand, Bright (1966) and Godsey et al. (2005) suggested that lake level remained near the Red Rock Pass threshold level until ~14 ka. Both lake-level model trajectories are illustrated in Fig. 2A.

3. Previous correlations of Bonneville levels with North Atlantic records of abrupt climate change

Oviatt (1997) correlated the initiation of the post-Provo recession of Lake Bonneville (Fig. 2A), which he placed at 14 ^{14}C ka (17 ka), with the termination of Heinrich event H1 and the Stansbury Oscillation, which he placed between 22 and 20 ^{14}C ka (26.4–23.9 ka), with the termination of Heinrich event H2. He, therefore, concluded that Heinrich events were followed by dry periods in the Bonneville lake basin. However, H1 has a GISP2-based age of 15.8 ka and, therefore, would appear to substantially post-date the Provo recession, given Oviatt's (1997) age determinations.

Oviatt et al. (2005) also correlated a ripple-laminated sand unit exposed on the northeast side of the Great Salt Lake with the Gilbert shoreline. Calibrated ^{14}C dates of plant fragments from this unit ranged in age from 12.9 to 11.2 ka and Oviatt et al. (2005) associated the Gilbert wet event with the Younger Dryas cold interval, which has an ice-core-based age of 12.9–11.6 ka (see, e.g., Stuiver et al., 1995).

4. Methods

4.1. Sediment coring

The Blue Lake core was taken from geothermally fed wetlands 27 km south of Wendover, Nevada, on the western edge of the Bonneville Basin (Fig. 1). Blue Lake Marsh is one of the largest (~18.5 km^2) wetland areas in the Great Salt Lake Desert. It is fed by upwelling groundwater from two principal spring-discharge areas, Lookout Point and Blue Lake. Lookout Point contains three springs, discharging approximately 11–17 L per second (L/s) from deep
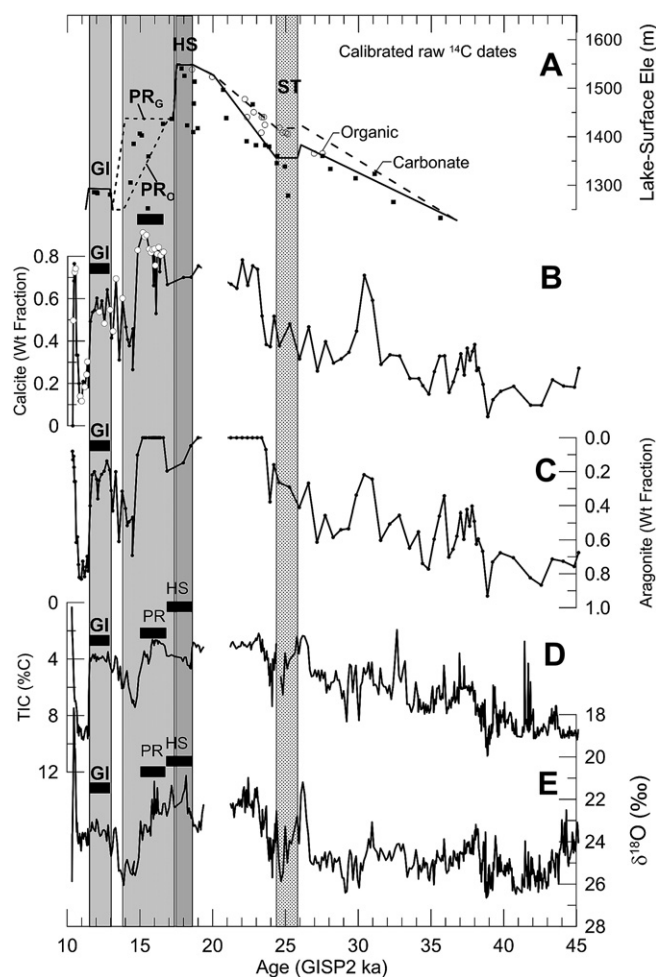

Fig. 2. (A) Lake-level envelope for Lake Bonneville (data from Oviatt et al., 1992), (B) fraction calcite, (C) fraction aragonite, (D) TIC (%C), and (E) δ^{18}O records from Blue Lake core BL04-4. GI = Gilbert stillstand, PR = Provo stillstand, HS = Bonneville highstand, ST = Stansbury Oscillation as indicated by data acquired from outcrop. The dashed line in (A) labeled PR$_O$ indicates the timing of the Provo event suggested by Oviatt (1997), whereas the dashed line labeled PR$_G$ represents the timing of the Provo event suggested by Godsey et al. (2005). The dashed line in (A) between 37 and 20 ka represents a possible lake-level trajectory during the Stansbury Oscillation, which is consistent with the dates of sub-Provo sediments on the Provo platform obtained by Sack (1999). Vertical gray-shaded rectangles enclose the Gilbert stillstand (Oviatt et al., 2005), the Provo stillstand as suggested by Godsey et al. (2005), the Bonneville highstand (Oviatt et al., 1992), and the Stansbury Oscillation (Oviatt et al., 1992) and reflect the shape of the lake-level envelope depicted in (A). The open circles in (B) between 17 and 10 ka indicate the presence of low-Mg calcite. Possible scenarios for the timing of the Bonneville highstand (HS) and Provo event (PR) are shown as sets of black rectangles.

extensional faults at the interface between Great Salt Lake Desert playa and the eastern edge of the carbonate (dolomites and limestones) Goshute Mountains. The Lookout Point Spring feeds several small ponds less than 1.5 m deep and 2500 m² in extent. Overflow from the ponds spreads to the southeast, forming very shallow, saline, water bodies typically less than 0.5-m deep. Surrounding marshlands are composed of a mosaic of bulrush-dominated marshes, small ponds (usually <10 m diameter), narrow sloughs, and saltgrass meadows. A much larger spring, Blue Lake Spring, discharges more than 100 L/s, primarily into Blue Lake, a large warm-water pond approximately 17 m deep and 0.04 km² in area. Blue Lake overflows into shallower pans and, ultimately, into the Great Salt Lake Desert playa.

This study included two sediment cores that were collected from the western lobe of the wetland system. The principal sediment core described in this report (BL04-4) comes from a sampling site (GPS coordinates, NAD83 datum, are 11T, 751157 E, 4487472 N) approximately 260 m southwest of Blue Lake. The site, at 1298 m above sea level (m.a.s.l.), consists of a moist, spongy peat vegetated in saltgrass. A second core (BL05-2) was collected 18 m south of BL04-4 on the north side of a small pond. During the formation of the Bonneville, Provo, and Gilbert shorelines, the core sites were covered by, respectively, 286, 176, and 5 m of water.

Sampling was conducted using a modified Livingstone piston corer with a 5-cm-diameter steel core barrel. Use of trade, product, or company name within this paper does not constitute an endorsement by the U.S. Government.

Core BL04-4 was taken manually and consists of nine drives with a total depth of 8.03 m from core top (8.58 cm from ground surface). A 55-cm-thick root plug was removed from the surface to facilitate coring. Core BL05-2 consists of seven drives with a total depth of 5.89 m. Drives were extruded into hard plastic sleeves for transportation to the Desert Research Institute laboratory in Reno, Nevada.

4.2. Development of age models

Radiocarbon (¹⁴C) ages of the total organic carbon (TOC) fraction of 19 samples from BL04-4 were determined by Beta Analytic (9 samples) and the Center for Accelerator Mass Spectrometry (10 samples) at the Lawrence Livermore National Laboratory

(Table 1). Radiocarbon ages of the TOC fraction of 6 samples from BL05-2 were determined by Beta Analytic (1 sample) and the Center for Accelerator Mass Spectrometry (5 samples) at the University of California-Irvine (Table 2). All ¹⁴C ages were calibrated using Calib 6.01 and IntCal09 (Stuiver et al., 2005).

Paleomagnetic studies of BL04-4 and BL05-2 were carried out using u-channel samples. U-channels are columns of sediment, 2 × 2 cm in cross-section taken from the middle of the split-face of each core segment and encased in plastic tubes. U-channel samples were taken from all core segments of BL04-4 (A–I) and from all segments of BL05-2 (A–H) except segments F (407–412 cm) and H (500–589 cm).

All u-channel paleomagnetic measurements were made using the automated 2G cryogenic magnetometer at the University of California-Davis. All magnetic measurements were made at 1-cm intervals; however, the magnetometer electronics impose a ~±3-cm smoothing of the magnetization at each sampling horizon. This causes the magnetic measurements to appear smoother than if successive 2-cm sediment cubes had been individually measured. However, the u-channel measurements are capable of resolving the paleomagnetic and rock magnetic variability used to correlate and date the Blue Lake sediment cores.

The natural remanent magnetization (NRM) of all u-channels was measured and then step-wise demagnetized in alternating magnetic fields (AF) of 10–60 mT in 10 mT steps and then remeasured. Anhysteretic remanence (ARM; 0.05 mT bias field, 100 mT AF) was then imparted to the u-channels and measured in the same manner as the NRM. Finally, an isothermal remanence (IRM, 1 T) was imparted to the u-channels and measured in the same manner as the NRM and ARM. The initial NRM, ARM, and IRM intensities for the two cores are shown in Supplementary Figs. 1 and 2. The pattern of intensity loss during AF demagnetization of the NRM, ARM, and IRM is illustrated in Supplementary Fig. 3 for twenty horizons in core 04–4, spaced about every 25 cm.

The NRM directional changes with AF demagnetization are small up to 40 mT. This is because NRMs have a stable characteristic remanence that yields coherent NRM directions between 5 and 40 mT. The NRM directions for the two cores are plotted in Figs. 3 and 4. Inclinations and declinations from several levels of AF demagnetization are plotted together to illustrate the coherence of the characteristic remanences. Several features in the directional (inclination, declination) and intensity changes (similar for NRM, ARM, and IRM) are identified and labeled in Supplementary Figs. 1 and 2 and Figs. 3, 4.

4.3. Sample preparation, isotopic, and mineralogical analyses

The BL04-4 core was subsampled continuously at 1-cm intervals from a depth of 186 cm below the ground surface to a depth of 856 cm. Proxy lake-size records were produced for the period 45.1–10.5 ka; therefore, each sample of lake sediment integrates, on average, ~50 y of record, assuming a constant sedimentation

Table 1
Calibrations of BL04-4 ¹⁴C ages using CALIB 6.01.[a]

Depth in core (m)[b]	Abs D (m)[c]	Lab no.	¹⁴C age B.P.	¹⁴C error y	Cal ka midpoint	Cal ka error
0.105	0.625	Beta-200218	1420	40	1.32	0.02
0.795	1.315	Beta-200219	2910	50	3.02	0.06
1.665	2.185	Beta-208405	5950	50	6.77	0.04
2.025	2.545	CAMS-121658	6690	30	7.57	0.01
2.555	3.075	Beta-197282	9590	50	10.85	0.06
2.560	*3.080*	*Beta-230619*	*7830*	*40*	*8.60*	*0.04*
2.775	*3.295*	*CAMS-117530*	*10040*	*60*	*11.53*	*0.13*
2.84	3.36	Beta-230853	9890	40	11.28	0.04
2.89	*3.41*	*Beta-231767*	*6830*	*40*	*7.65*	*0.03*
3.02	*3.54*	*Beta-230854*	*13860*	*60*	*16.93*	*0.09*
3.325	3.845	CAMS-121659	13550	40	16.74	0.09
3.610	4.130	CAMS-121660	15750	45	18.86	0.10
4.175	4.695	CAMS-121661	19250	60	22.89	0.25
4.555	5.075	CAMS-121662	22550	80	27.30	0.29
4.815	*5.335*	*Beta-200220*	*18440*	*60*	*22.05*	*0.20*
5.635	6.155	CAMS-121663	30300	200	34.84	0.14
6.360	6.880	CAMS-117531	34560	380	39.55	0.54
6.947	7.467	CAMS-117532	37110	520	41.94	0.38
7.645	8.165	CAMS-121664	40200	650	44.10	0.53

[a] Samples in italics are out of stratigraphic order.
[b] Depth in core refers to depth below top of drive A.
[c] Absolute depth refers to depth below top of marsh.

Table 2
Calibrations of BL05-2 ¹⁴C ages using CALIB 6.01.[a]

Depth below C (m)[b]	Core D (m)	Lab no.	¹⁴C age B.P.	¹⁴C error y	Cal ka midpoint	Cal ka error
1.225	2.985	Beta-238793[c]	9710	50	11.16	0.05
1.335	3.095	UCIAMS-48200	9895	25	11.27	0.02
1.585	*3.345*	*UCIAMS-48201*	*12600*	*35*	*14.94*	*0.14*
1.815	3.575	UCIAMS-48202	10480	25	12.49	0.03
2.055	*3.815*	*UCIAMS-48203*	*13765*	*50*	*16.87*	*0.08*
2.245	4.005	UCIAMS-48204	12085	30	13.93	0.07

[a] Samples in italics are out of stratigraphic order.
[b] Depth below C refers to depth below top of drive C.
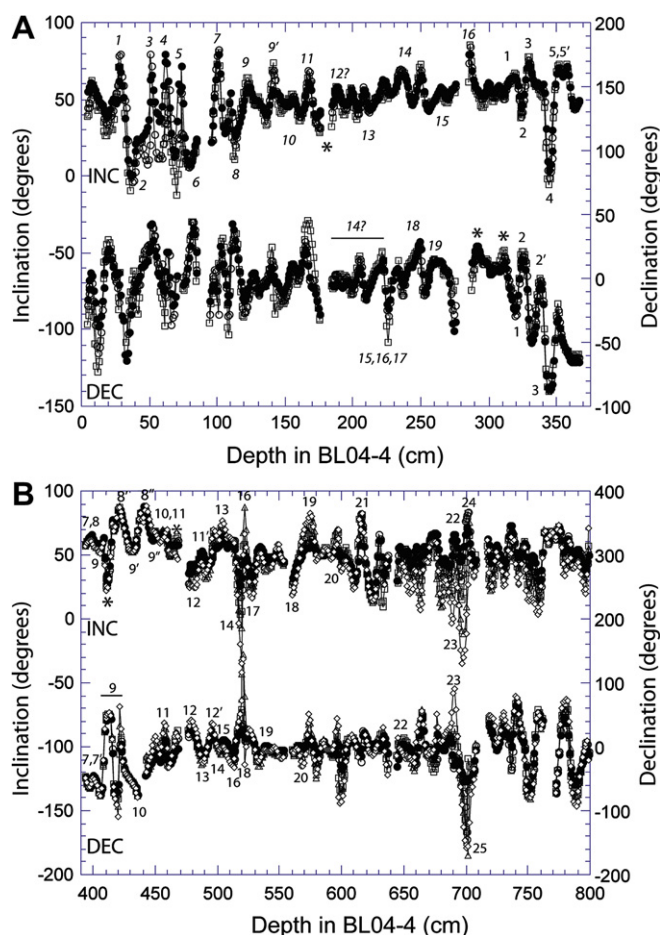[c] The Beta-238793 sample came from the base of the accumulated peat.

Fig. 3. A. BL04-4 inclination and declination values between 0 and 375 cm. B. BL04-4 inclination and declination values between 390 and 800 cm. The symbols represent inclination and declination values after different levels of alternating-field demagnetization (5–25 mT). The italicized numbers (1–19) are inclination or declination features noted and dated in other North American lakes (Lund, 1996). The non-italicized numbers (at deeper depths in BL04-04) are inclination or declination features noted and dated in North Atlantic Ocean marine sediments (Lund et al., 2001a,b; see Supplementary Figs. 4 and 5).

rate. Given the time span of the studied core (∼35 ka), these records are considered to be highly resolved. The upper part of drive E in BL04-4 (3.70–3.90 m) was "slop" (sediment that flowed into the core hole at the base of a drive and that was re-cored during a subsequent drive) generated during the coring process. The data generated from this sediment was not used in this study and that interval was treated as an artificial gap.

Prior to isotopic and coulometric analyses, organic carbon was removed from each sample by adding 20 ml of a 50% solution of bleach to a 40-ml centrifuge tube, containing the sediment sample. The bleach was used to remove labile organic carbon compounds that could distort the $\delta^{13}C$ values of the TIC fraction. The sample was shaken and allowed to stand overnight. The sample was centrifuged for 15 min at 20,000 rpm using a Sorval Superspeed RC2B and the supernatant discarded. In order to remove soluble salts, the sample was combined with deionized water, shaken and centrifuged, conductivity of the supernatant measured, and the supernatant discarded. This procedure was repeated until the specific conductivity of the supernatant was <3 times the conductivity value of tap water at the U.S.G.S. Boulder, Colorado laboratory. The sample was then freeze-dried and homogenized.

BL04-4 samples were analyzed for $\delta^{18}O$ and $\delta^{13}C$ using a Micromass Optima gas-source triple-collector mass spectrometer
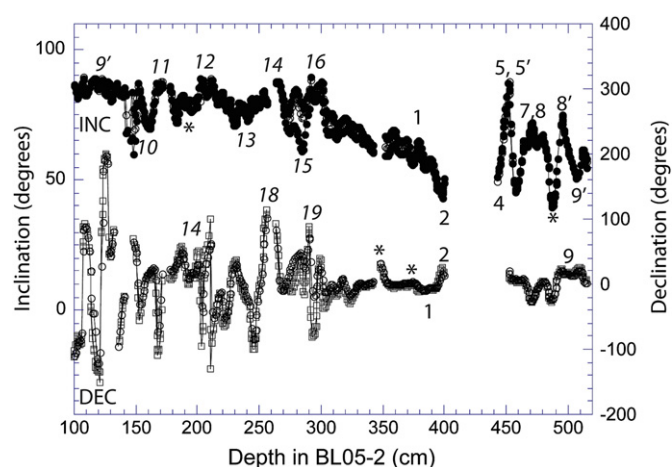

Fig. 4. BL05-2 inclination and declination values between 100 and 520 cm. Symbols and numbers are the same as noted in Fig. 3.

equipped with a dual inlet and interfaced with a MultiPrep automated sample preparation device. The precision (one sigma) of analyses of reference standard NBS-19 is estimated to be ±0.04‰ for $\delta^{18}O$. The precision of analyses of sediment samples is estimated to be ±0.2‰ for $\delta^{18}O$. Measurements of TIC were done using a UIC model 5011 CO_2 Coulometer outfitted with a UIC model 5030 Carbonate Carbon apparatus. The precision (one sigma) of the TIC analyses is ±0.1%.

Slurry mounts of 254 powdered samples were prepared on glass slides and analyzed on a Rigaku Multiflex X-ray diffractometer using Cu Kα radiation. All samples were scanned from 20 to 40° 2θ and 12 samples were scanned from 3 to 60° 2θ. Identification of minerals and determination of their abundances was based on peak height and peak area relative to background for quartz (26.66° 2θ), calcite (29.41° 2θ), dolomite (30.86° 2θ), and aragonite (27.25° and 33.18° 2θ). Relative peak height and area proportions were calculated by dividing the peak height/area for each mineral (two peaks/areas for aragonite) by the sum of all five measured peak heights/areas. The relative peak proportion (rpp) for each mineral was determined as the average of the relative peak height and relative peak area. Mineral percentages were determined by comparison with prepared standards; e.g., calcite = 0.64 × rpp (calcite).

The TIC analyses were used to transform the X-ray-based relative abundances of calcite, dolomite, and aragonite into absolute abundances. Samples were analyzed by X-ray diffraction (XRD) between 186 and 287 cm at 20-cm intervals, between 287 and 303 cm at 5-cm intervals, between 303 and 403 cm at 1–2 cm intervals, between 403 and 653 cm at 5-cm intervals, and between 653 and 856 cm at 20-cm intervals. Low-magnesium (Mg) calcites were defined as having 2θ values >29.7. All isotopic, chemical, and mineralogical data for BL04-4 samples are listed in Supplementary Table 1. 2θ values have been listed for BL04-4 samples only.

4.4. Sedimentological analyses

The sedimentary analysis is primarily based on observations of a continuous series of u-channel samples from BL04-4. The samples had dried, but they still could be correlated to photographs of the fresh core to provide accurate depth control. Each sediment sample was scraped smooth, using a straight razor, and examined with a zoom stereoscopic microscope up to a magnification of 60×. Smear-slide samples were collected with a dissecting needle at irregular intervals and were examined with a petrographic microscope at a magnification of 400×.

5. Results and discussion

The following presents the results of the paleomagnetic, sedimentologic, mineralogic, and chemical studies.

5.1. Paleomagnetic secular variation applied to BL04-4 and BL05-2

The inclination and declination variability in the Blue Lake cores are correlated with two different sets of dated PSV records from other parts of North America. The first set (Lund, 1996) is derived from Holocene PSV (0–10 ka) records in North American lakes where 14 inclination features and 17 declination features are identified and dated based on multiple, independent radiocarbon-dated records (data not illustrated in this paper). The second set (Supplementary Fig. 4) is derived from Late Pleistocene deep-sea PSV records from the North Atlantic Ocean that cover the interval 10–70 ka (Lund et al., 2001a, 2001b; Lund and Keigwin, 1994). The inclination (I) features are numbered 1–47 and the declination (D) features are numbered 1–49. The data are plotted versus calendar time based on the GISP2 chronology. The tie to the GISP2 chronology was determined using oxygen-isotope data, TIC data, and distinctive sedimentological variability in the deep-sea cores (Johnson et al., 1988; Keigwin and Jones, 1994).

The paleomagnetic data in Figs. 3 and 4 were tied to the numbered and dated master lake and master deep-sea PSV features using the following procedure. The ^{14}C dates suggest that Blue Lake has a nearly complete Holocene and Glacial Transition record. A consistent correlation between the master marine and master lake PSV records was found and those matching features have been numbered in Figs. 3 and 4. The numbered features are individual inclination or declination features that are visible in both BL04-4 and BL05-2 and present in the master records. The inclination and declination features occur in consistent stratigraphic order (in all records). On occasion, declination features were present in one Blue Lake core but not the other. These inconsistencies are interpreted to stem from small differences in lithology (e.g., local unconformities), coring-related deformations, and problems with u-channel measurements made near drive boundaries where intensity variability is large. As part of this exercise, the ^{14}C record was used to estimate the approximate depth interval in the core that should host the Mono Lake and Laschamp excursions. A set of inclination and declination features thought to best fit both excursions were found within the postulated depth intervals. Then a consistent set of PSV features were documented that occur between the Mono Lake Excursion and the Glacial Transition and that occur between the Mono Lake and Laschamp magnetic excursions (Lund et al., 1988, 2005).

In Fig. 5 correlatable inclination and declination features normalized to depth in BL04-4 are plotted. The ages of these features are based on correlations between the Blue Lake PSV records and the master lake and deep-sea PSV chronologies. Also plotted in Fig. 5 are the depths and ages of 14 in-stratigraphic-order ^{14}C dates obtained on BL04-4 (out of order dates were eliminated in this plot but are shown in Supplementary Fig. 5). With one exception, the calibrated ^{14}C ages are in overall agreement with the PSV GISP2-based chronology. The PSV chronostratigraphy, however, exhibits much greater detail in the time-depth sense than the ^{14}C data alone. Supplementary Figs. 5 and 6 indicate piecewise-continuous age models for BL04-4 and BL05-2. A linear extrapolation from the oldest PSV-available data point at 42 ka–45 ka at 8 m is based on the trajectory of the oldest two calibrated ^{14}C dates, which span this range (Supplementary Fig. 5); i.e., the PSV age model was extrapolated parallel to the trajectory of the two ^{14}C dates.

A comparison of the calibrated ^{14}C data with the PSV age model for BL05-2 indicates that sediments deposited between 17 and
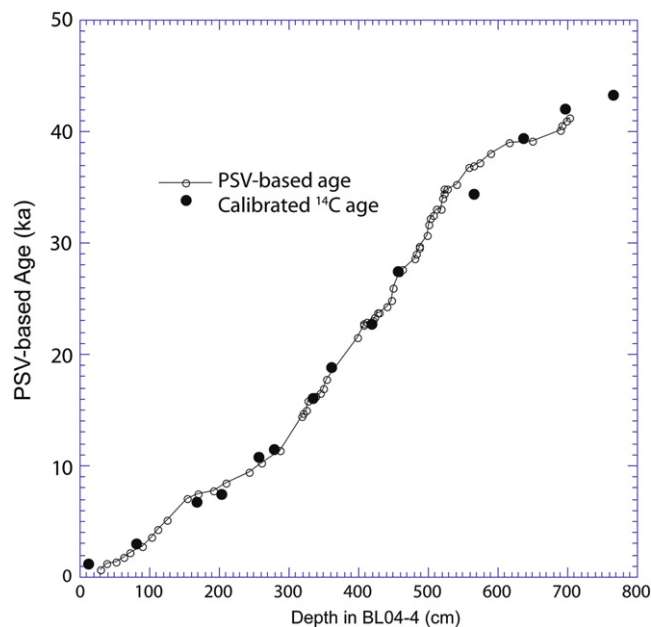

Fig. 5. Open circles represent ages of BL04-4 inclination and declination features plotted as a function of depth and filled circles indicate stratigraphically-in-order calibrated ^{14}C ages of samples from BL04-4 plotted as a function of depth.

12 ka experienced a great deal of reworking. Core BL05-2 was included in this study because of its relatively high sedimentation rate; i.e., it was hoped that it would reveal a more detailed record of the fall from the Bonneville highstand. However, given complications associated with sediment reworking, further discussion of data obtained on this core is excluded.

5.2. Comparison of the carbonate mineralogy, TIC concentration, and $\delta^{18}O$ records from BL04-4 with the outcrop-based lake-level envelope for the period 45–10 ka

With respect to carbonate mineralogy, the transition from low-Mg calcite to high-Mg calcite and from high-Mg calcite to aragonite is interpreted as reflecting a progressive increase in lake salinity and magnesium (Mg) concentration (see, e.g., Stanley et al., 2002 and references therein), which, therefore, reflects a reduction in lake volume.

In a relatively simple hydrologic system, TIC also can be used to estimate lake size; i.e., in a hydrologically closed system, the relative concentration of TIC should decrease as lake size increases. This is because in many Great Basin surface-water systems the flux of siliciclastic material to a lake is an exponential function of discharge, whereas the flux of Ca^{2+} (which combines with CO_3^{2-} to form $CaCO_3$ a major component of TIC) to the lake is a linear function of discharge (Benson et al., 2002). In a hydrologically closed lake, TIC will tend to decrease with increasing lake volume and should rapidly decrease when the lake overflows (see, e.g., Benson and Thompson, 1987: p. 671).

There are several factors that determine the $\delta^{18}O$ value of carbonate deposited from lake water; however, the most important factors are the $\delta^{18}O$ value of river discharge entering the lake and the $\delta^{18}O$ value of water vapor exiting the lake's surface. In general, the lake at hydrologic and isotopic steady state will have a $\delta^{18}O$ value equal to the $\delta^{18}O$ value of river discharge minus the $\delta^{18}O$ value of isotopically fractionated water vapor. A rising hydrologically closed lake will be associated with decreasing $\delta^{18}O$ values as will a hydrologically open lake, which experiences an increasing

rate of overflow and, therefore, a decreasing level of isotopic fractionation via evaporation (see, e.g., Benson and Paillet, 2002).

The Blue Lake core site (Fig. 1) in the Bonneville Basin has the advantage of being distant from past sources of glacial sediment. This implies that the Blue Lake TIC record should not have been strongly affected by the introduction of glacial rock flour that occurred during the past extensive glaciations of the Wasatch and Uinta Mountains which are on the eastern side of the basin.

Fig. 2A shows the lake-level envelope constructed for Lake Bonneville based on data from Oviatt et al. (1992). The dashed line labeled PR$_O$ indicates the decline in Lake Bonneville from the Provo shoreline suggested by Oviatt (1997), whereas the dashed line labeled PR$_G$ represents the extended occupation of the Provo shoreline suggested by data assembled by Godsey et al. (2005).

Also shown in Fig. 2 are four proxies of lake size: weight-fraction calcite (Fig. 2B), weight-fraction aragonite (Fig. 2C), TIC (as %C) (Fig. 2D), and δ^{18}O (Fig. 2E). During the Stansbury Oscillation there were two maxima in TIC and δ^{18}O at 25 and 24 ka (Fig. 2D, E), indicating the presence of two hydrologic oscillations. The TIC and δ^{18}O records indicate that the Stansbury Oscillation(s) began ~26 ka and ended ~23 ka. The decrease in TIC and δ^{18}O at 18.5 ka (Fig. 2D, E) are interpreted to indicate the time that Lake Bonneville began to overflow. Oxygen-isotope minima between 18.5 and 17.0 ka indicate rapid overflow of Lake Bonneville (Fig. 2E). Between ~23 ka and the beginning of Bonneville overflow at 18.5 ka, the calcite fraction (Fig. 2B) increased at the expense of aragonite (Fig. 2C), which indicates a lake that was increasing in volume, becoming more dilute. A rapid decrease in TIC (Fig. 2D), a minimum in δ^{18}O (Fig. 2E), and the initiation of low-Mg calcite precipitation (Fig. 2B) at 17.0 ka, together indicate the fall of Lake Bonneville to the Provo level and its subsequent rapid spill at that level. At 15.9 ka low-mg calcite precipitation ceases (Fig. 2B), TIC precipitation increases (Fig. 2D), and δ^{18}O values sharply increase (Fig. 2E). This suggests a brief oscillation of the lake beneath the Provo level, followed by a decreased rate of spill across the Provo threshold.

Between 15.2 and 14.7 ka, calcite decreased (with low-Mg calcite giving way to high-Mg calcite), aragonite increased, TIC increased, and δ^{18}O values increased sharply, indicating a fall from the Provo level and a return to closed-basin conditions (Fig. 2B–E).

The core-based timing of the Bonneville highstand and Provo events is not totally compatible with the lake-level envelope created by Oviatt et al. (1992) and (or) modified by Godsey et al. (2005). In particular, the termination of the Provo event at ~15.2 ka falls between both the Oviatt and Godsey models (Fig. 2). However, the timing of the fall from the Provo level is consistent with the findings of Hart et al. (2004) who used ^{87}Sr/^{86}Sr ratios of fish remains from Triple Barrel and Raven caves to show that Lake Bonneville was above 1325 m at 13.47 ± 0.10 and 12.91 ± 0.5 ^{14}C ka (16.6 ± 0.2 and 15.4 ± 0.2 ka).

The existence of a closed-basin lake after 14.9 ka is supported by enriched δ^{18}O, elevated TIC and aragonite values, and depressed calcite values between 14.9 and ~13.3 ka (Fig. 2B–E). These parameters plateaued between 13.1 and 11.6 ka at values indicating the existence of a relatively large body of water; i.e., the Gilbert Lake. The fall from the Gilbert shoreline, indicated by rapid increases in aragonite, TIC, and δ^{18}O and a decrease in calcite appears to have occurred at 11.5 ka.

There are abrupt decreases in calcite, TIC, and δ^{18}O at 10.5 ka. The authors suggest that this was not related to Lake Bonneville, which by this time had retreated from the core site. Instead, this represents a period of low-Mg calcite precipitation from groundwater spring discharge at the Blue Lake marsh site. The existence of a marsh environment at the core site between 11.5–10.3 ka is supported by the existence of water-laid sediments composed of bioturbated aragonite mud in the bottom part of the interval that were deposited in a wet marsh environment. As pointed out in Section 5.4 below, the top of the 11.5–10.3 ka interval contains roots and other soil features that are also indicative of a marsh environment. Thus, a deep lake interpretation for the low δ^{18}O values at 10.5 ka can be ruled out.

5.3. Environmental sedimentology of BL04-4

Fig. 6 depicts the sedimentology and smear-slide mineralogy of BL04-4. The desiccated condition of the core made it difficult to obtain samples that contained only one form of carbonate; i.e., almost every slide contained a mixture of calcite and aragonite. Therefore, the carbonate mineralogy indicated in Fig. 6 represents the dominant carbonate phase within a particular sedimentary interval. Supplementary Table 2 lists generalized descriptions of the sedimentary intervals in BL04-4 as well as interpretations of their environmental setting.

Core BL04-4 possesses seven sediment groupings: peat with silt, calcite with woody stems, burrowed calcite with pebbles and sand, laminated carbonate mud, pelleted aragonite mud with calcite laminae, burrowed aragonite mud, and aragonite mud with sand beds composed of quartz and pellets.

Peat containing silt beds dominate the upper part of the core. The peat beds contain carbonaceous roots and hollow, woody plant stems. The peat intervals likely formed under environmental conditions similar to those occurring in the modern Blue Lake marsh.

The calcite-with-woody-stems grouping occurs interbedded with the peat and also can be found between 329 and 288 cm (15.64–11.53 ka) in the core. This grouping commonly contains abundant diatoms and ostracodes as well as carbonaceous root casts. Snails are also abundant in some parts of this grouping. The woody stems are very similar to those found within the peat fabric. This grouping may represent spring-fed pools or the shallow margin of a calcite-precipitating lake whose sediments were later penetrated by the roots of plants growing in a marsh environment.

Burrowed, calcite-rich units contain "floating" pebbles and sand- to granule-sized quartz. Ostracodes are present in some places and diatoms are often present but not abundant. This grouping is interpreted to indicate a well-mixed lake from which calcite precipitated. The quartz pebbles and sands were probably delivered from ice cover or via ice rafting and make up 1–2% of the sediment.

The laminated carbonate mud is mostly composed of aragonite. Flat layers of silt or very-fine sand, overlain by carbonate mud comprise the most common laminae. A laminated calcite mud occurs between 362 and 350 cm (18.64–16.78 ka), and laminated aragonitic mud occurs between 443 and 422 cm (24.86–23.25 ka), between 718 and 694 cm (41.90–40.57 ka), and between 803 and 790 cm (45.13–44.62 ka). These intervals were deposited in a lake that received intermittent fluxes of coarser sediment, and the layering may represent a flushing of streams that entered the lake. The dearth of bioturbation within the laminated aragonite mud may indicate stratified lake conditions or rapid sedimentation. Between 499 and 456 cm (31.36–26.63 ka), some of the thinnest laminae, consisting of aragonite mud alternating with organic material, occur. These laminae may represent chemical precipitation from the epilimnion of a stratified lake, which alternate with algal material.

Pelleted aragonite mud contains well-rounded, ovate clumps of aragonite that are 1–2 mm in length and <1 mm in diameter. The most common occurrence of this grouping occurs as irregular-shaped aragonitic laminae, containing abundant "floating" pellets which alternate with aragonite mud containing few or no pellets. Dark-gray calcitic mud forms irregular 0.5- to 2.0-cm-thick layers within this grouping. The layering within this grouping is interpreted to indicate the deposition of brine shrimp pellets followed
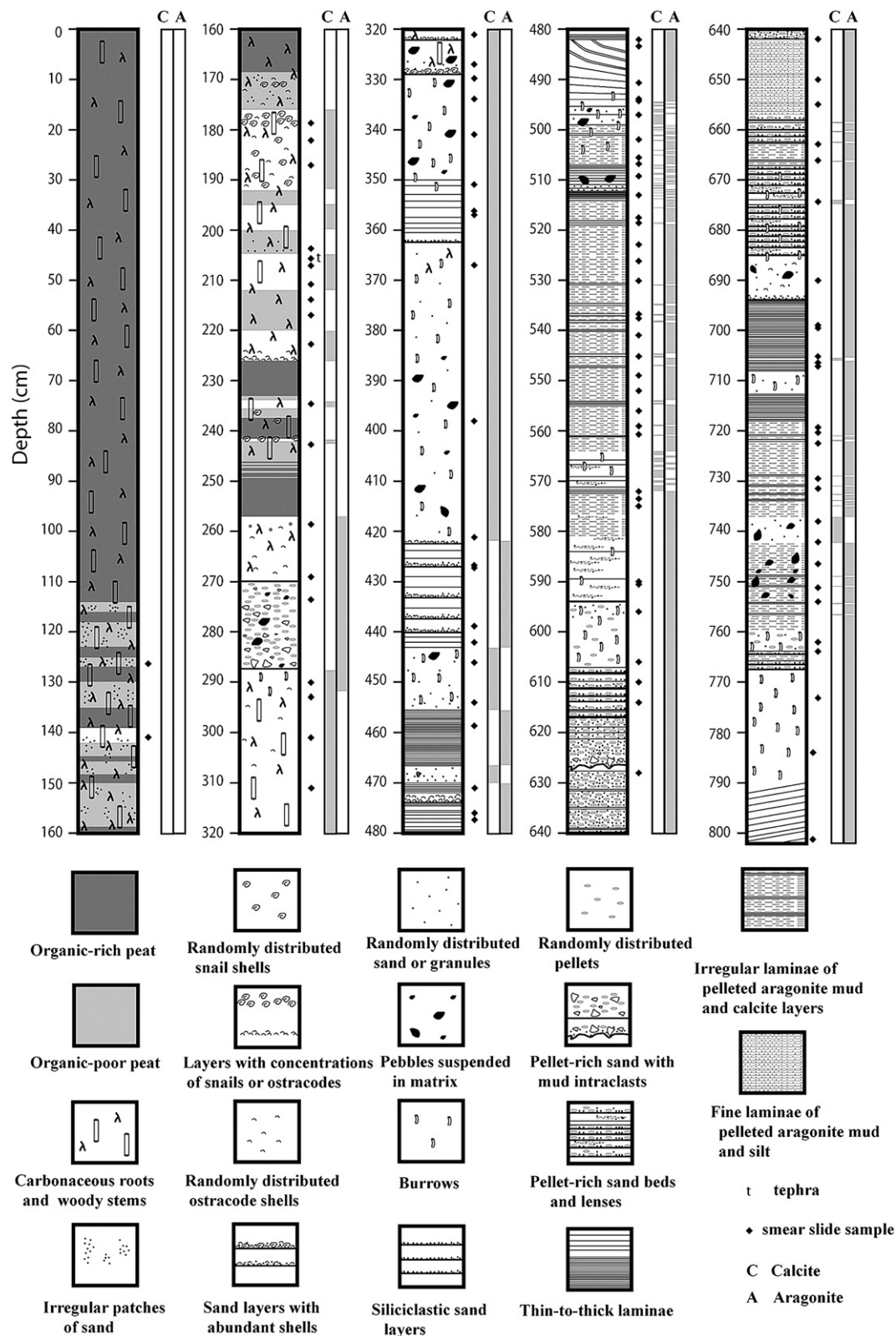
Fig. 6. Stratigraphic section for BL04-4.

by intermittent wave resuspension of fine-grained sediment, which concentrated the pellets. The presence of brine shrimp suggests that the lake was fairly saline. Bioturbation is generally subdued and restricted to bedding planes, which may indicate the existence of a stratified lake with anoxic lake-bottom sediments. The

formation of calcite layers is interpreted to result from periods of fresh-water influx, which diluted the lake's epilimnion. Pebbles, quartz sand, and granules occur within pelleted aragonite laminae between 759 and 742 cm (43.45–42.81 ka), suggesting the presence of ice cover or ice rafting.

Burrowed (bioturbated) aragonitic mud lacking layers is found throughout several intervals within the core. Some of the massive aragonite mud contains pellets (607–594 cm, 764–759 cm) (38.38–38.07 ka, 43.68–43.45 ka) and some contains scattered quartz sand (694–685 cm, 712–708 cm) (40.57–40.13 ka, 41.68–41.53 ka) or quartz silt (790–768 cm) (44.62–43.79 ka). In all cases, the aragonite mud is interpreted to have been deposited in a fully oxygenated lake, which allowed burrowing organisms to feed at the lake bottom. Sedimentary intervals which contain pellets indicate elevated lake salinity. Aragonite mud with layers of siliciclastic sand is sometimes found mixed with aragonite pellets. The sand layers have sharp, flat bases and abrupt caps, and some of the layers are lenticular in shape. Two layers at 288–270 cm (11.53–10.60 ka) and at 638–621 cm (38.91–38.64 ka) contain very coarse sand, pebbles, and abundant mud intraclasts. Both of these layers are graded. The sand layers are interpreted to have resulted from waves generated during storms, and the graded layers were deposited with near-shore transgressive gravels.

Interpretation of the Blue Lake 04-4 sedimentary sequence is somewhat difficult due to the desiccation of the core and the small diameter of the u-channel. The mixture of calcite and aragonite in most smear-slide samples can be interpreted as evidence of reworking of older deposits throughout the history of deposition. Alternatively, the mixture may simply reflect the "dragging" of one layer's mineralogy to another layer, during the surface-cleaning (scraping) process. In any case, there is a good fidelity between mineralogy and sedimentary fabric, suggesting that the mixing has not masked the primary depositional signal.

There is one depth at which an erosional gap exists; i.e., at the base of the pelleted sand at 288 cm (11.53 ka). The radical change in mineralogy and depositional style, as well as the occurrence of mud intraclasts in the sand, indicate erosion. These fabrics are interpreted to indicate the subaerial exposure of lake sediment followed by the formation of a shallow aragonite-precipitating water body over older calcite-precipitating lake sediment. Other sandy intervals within the core probably indicate some loss of material, but at a very local scale.

5.4. Comparison of the BL04-4 $\delta^{18}O$ record with its sedimentological record

The following is a condensed lake history extracted from observed sedimentary fabrics in BL04-4 (see Fig. 6 and Supplementary Table 2)

1. 803–764 cm (45.1–43.7 ka) – A lamination-producing deep lake shallowed to a bioturbated shallow lake; waves then reworked the brine shrimp pellets deposited in the shallow lake.
2. 764–737 cm (43.7–42.7 ka) –The lake became progressively deeper and fresher, recorded by the transition from a bioturbated, pelleted aragonite to a laminated, pelleted aragonite-containing calcite interbeds, followed by the deposition of a calcite mud. Ice-forming conditions prevailed through the younger part of this sequence.
3. 737–685 cm (42.7–40.1 ka) – The laminated pelleted aragonite mud at the base of this interval indicates an abrupt decrease in lake size. The lake gradually became deeper, leading to deposition of a laminated aragonite mud. The bioturbated aragonite mud indicates a decrease in lake-size followed by an increase in lake level indicated by a return to deposition of laminated sediment.
4. 685–642 cm (40.1–39.0 ka) – The lake fell rapidly, depositing a pelleted aragonite that was wave-reworked. The lake then deepened gradually, first depositing a laminated, pelleted aragonite, then depositing a thinly laminated aragonite, which also contains sand laminae.

5. 642–627 cm (39.0–38.7 ka) – Lake-level fell, and a wave-reworked, pelleted aragonite was deposited.
6. 627–594 cm (38.7–38.1 ka) – A rising-lake sequence from a pellet-rich sand to bioturbated, pelleted aragonite mud.
7. 594–507 cm (38.1–32.5 ka) – A rising-lake sequence, starting with a wave-reworked, pelleted aragonite formed in a shallow lake and then transitioned to a laminated, pelleted aragonite that formed in a deep lake. At the top of this interval, there is laminated aragonite mud and a calcite mud with drop stones that indicate relatively high lake levels.
8. 507–497 cm (32.5–31.1 ka) – The lake fell, depositing pelleted aragonite and then rose, indicated by precipitation of calcite which contains ice-related drop stones.
9. 497–470 cm (31.1–28.2 ka) – The lake became more saline, depositing aragonite. It then became stratified, producing an organic laminate. A turbidite near the top of the interval was created by wave reworking of older, higher-elevation deposits.
10. 470–456 cm (28.2–26.6 ka) – The lake transgressed and drop-stone-containing calcite was precipitated. A rapid drop of lake level then occurred with the consequent formation of an organic laminate.
11. 456–422 cm (26.6–23.4 ka) – First, a rise in lake level occurred and a drop-stone-containing calcite precipitated from the deep lake; lake level then fell and a laminated aragonite was deposited, possibly from a stratified lake.
12. 422–329 cm (23.4–15.6 ka) – A thick interval of calcite containing drop stones was precipitated from a deep lake. The laminated calcite interval between 362 and 350 cm (18.6–17.0 ka) indicates a very deep lake.
13. 329–288 cm (15.6–11.5 ka) – These sediments contain a falling lake sequence. There are beds of shells which indicate wave reworking or they may indicate wave-generated turbidites. Towards the top of this interval, the presence of roots and woody stems suggests a shallow, lake-margin environment.
14. 288–258 cm (11.5–10.3 ka) – This interval indicates water-laid sediments that were deposited after subaerial exposure at 288 cm. The water-laid sediments are composed of bioturbated aragonite mud possibly deposited in a wet marsh environment. The top of the interval contains roots and other soil features that indicative of a marsh environment.
15. 258–0 cm (10.3–1.0 ka) – These are fresh-water marsh deposits with the organic-poor intervals indicating pools of standing water. There is a volcanic ash at 204 cm that is thoroughly mixed with sediment. Louderback and Rhode (2009) have suggested that this volcanic ash is the Mazama tephra.

Interpretations of relative changes in Lake Bonneville levels from the sediment fabric study are largely in agreement with the $\delta^{18}O$ record of lake-level change (Fig. 2E). Of the 15 changes in the lake's hydrologic state suggested above, 12 (all but 2, 7, and 13) are in full agreement with the $\delta^{18}O$ proxy lake-level record. In addition, the Stansbury Oscillation(s) (26.0–23.0 ka) is indicated by a lake-level oscillation in the sedimentary record (4.51–4.14 m); the Bonneville highstand which is thought to have started at 18.5 ka is signaled by the initiation of laminated calcite precipitation (3.6 m); the fall from the highstand at 17.0 ka to the Provo level is indicated by termination of laminated calcite precipitation (3.5 m); the fall from the Provo level beginning at ~15.2 ka is indicated by a layer of sand and shells (3.24 m) that probably represent deposition of wave-formed turbidites that occurred during a fall in lake level. The fall from the Gilbert level at 11.6 ka, is evidenced by an erosional surface and root penetration of Gilbert sediments subsequent to subaerial exposure (2.88 m). However, the rise in lake level prior to the Gilbert is not clearly indicated in the sedimentary record.

When Lake Bonneville was at the Gilbert level, only 5 m of water covered the core site (elevation = 1298 m). Oviatt et al. (2005) have indicated that Lake Bonneville would have declined from the Provo level to an elevation ~11 m below the subsequent Gilbert level. This suggests that Lake Bonneville should have fallen below the Blue Lake site sometime between 14.7 and 13.1 ka (in BL04-4). As BL04-4 sediments do not indicate subaerial exposure of the site during the 3.22- to 3.06-m depth interval (Fig. 6), it is suggested that the site was covered by a wet marsh within which was deposited the carbonaceous roots and woody stems typical of this sedimentary interval (Fig. 6). The aragonitic lake sediments that post-date this sequence may have been deposited in a shallow lake that locally occupied the Bonneville Desert.

Fig. 7 highlights the carbonate mineralogy and $\delta^{18}O$ records from BL04-4 for the period ≤16−>6 ka. The fall from the Provo level occurs between 15.2 and 14.7 ka (signaled by an increase in TIC, $\delta^{18}O$, $\delta^{13}C$, and aragonite). The Bølling-Allerød warm interval (14.7–13.3 ka) is characterized by very low lake levels that increase irregularly over time, reaching a maximum during the Gilbert event
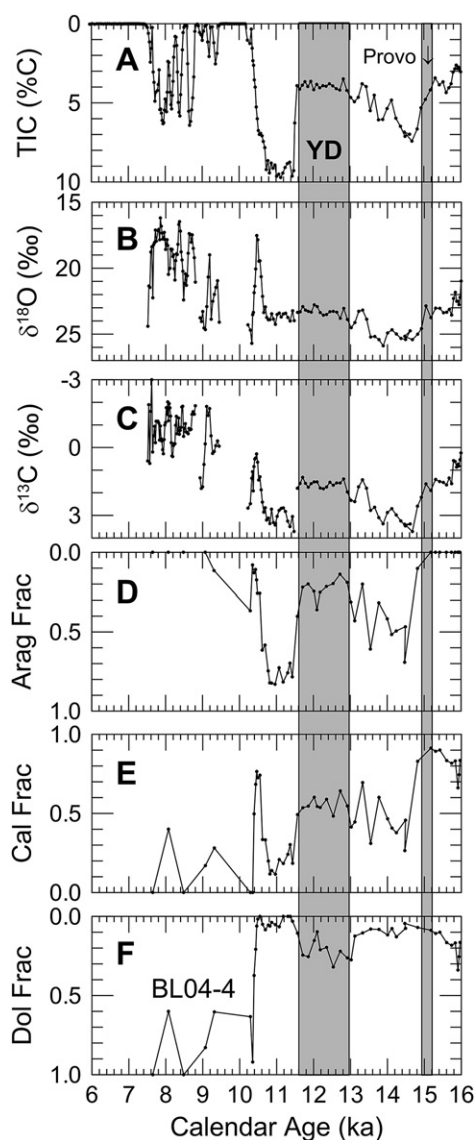
(Younger Dryas cold interval: 12.9–11.6 ka). During the early part of the Holocene (11.6–10.5 ka), lake level was very low and it is not clear whether Lake Bonneville was present at the core site or whether a localized body of water existed there. In any case, the withdrawal of Lake Bonneville from the Blue Lake area occurred on or before ~10.5 ka, and the existence of a spring-fed marsh was signaled by the initial production of calcite with $\delta^{18}O$ values that are much more depleted than pre-Provo values.

5.5. BL04-4 hydrologic-balance proxy records compared with the GISP2 ice-core $\delta^{18}O$ record

In Fig. 8, three lake-size proxies from BL04-4 are compared with the GISP2 $\delta^{18}O$ record, a proxy for North Atlantic air temperature. The GISP2 $\delta^{18}O$ record (Fig. 8A) has been labeled with Heinrich events H1-H4, Dansgaard-Oeschger events DO 1–12, the Bølling/Allerod (BØA) warm interval, the Younger Dryas (YD) interval, and
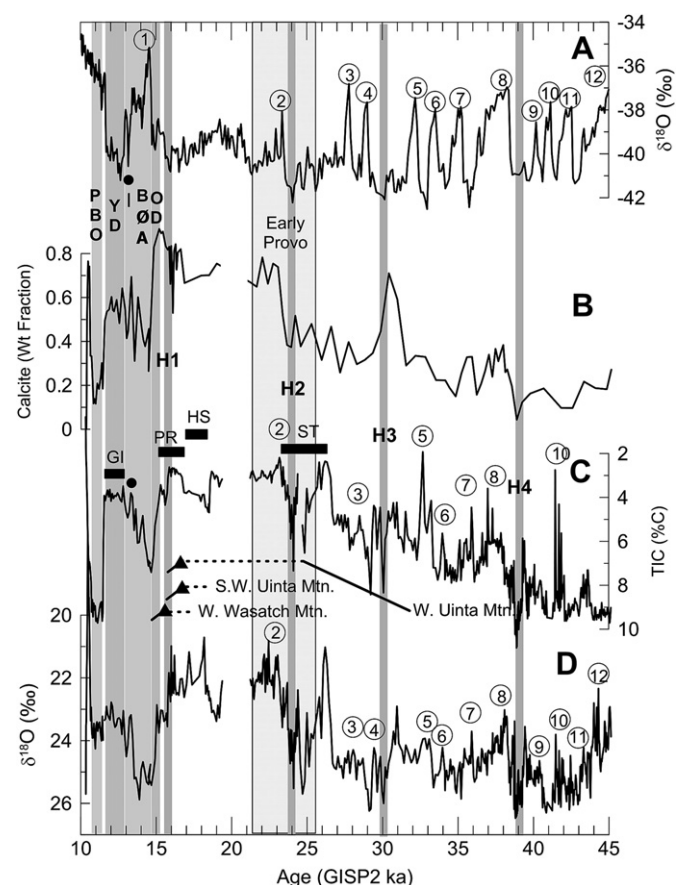
Fig. 7. BL04-4 hydrologic-balance proxy records for the period 16−6 ka. Vertical gray rectangle labeled YD indicates timing of Younger Dryas interval. Thin vertical rectangle with Provo ↓ to its left indicates fall from Provo event.

Fig. 8. Blue Lake core BL04-4 proxy lake-size records for (B) calcite, (C) TIC, and (D) $\delta^{18}O$ compared to the GISP2 $\delta^{18}O$ record (A). BØA refers to the Bølling/Allerød interval; YD refers to the Younger Dryas interval, PBO refers to the Pre-Boreal Oscillation, and" I" with a black dot refers to the Inter-Allerød cool period. Circled numbers in (A) refer to DO interstadials and H refers to Heinrich events. Gilbert stillstand, Provo stillstand, Bonneville highstand and Stansbury Oscillation denoted by solid black rectangles are labeled, respectively, GI, PR, HS, and ST. The timings of the hydrologic events were taken from the lake-size proxy records. The "early Provo" interval enclosed in the dotted rectangle is based on calibrated dates from sub-Provo sediments obtained by Sack (1999). The youngest sub-Provo date (21.1 ± 0.3 ka) occurs after the Stansbury event, probably reflecting the contamination of this sample with modern carbon. Increase in the extent of western Uinta Mountain glaciation is denoted by a solid black line; dashed line indicates time during which the glacier was near its farthest down-valley extent. Solid black triangles indicate mean ages of moraines. Circled numbers in (C) and (D) indicate possible correlations between DO events in the GISP2 core and $\delta^{18}O$ minima in BL04-4. Gray vertical rectangles indicate timing of climate events documented in Greenland Ice cores and North Atlantic sediments.

the Pre-Boreal oscillation (PBO). The durations of the North Atlantic climatic phenomena are shown as shaded rectangles. The timing of the Gilbert (GI) event, Provo (PR) event, the Bonneville highstand (HS) and the Stansbury Oscillation(s) (ST), as defined by new data introduced in this paper, are shown as black rectangular bars (Fig. 8C). In addition, an "early Provo" interval based on calibrated dates from sub-Provo sediments (Sack, 1999) is indicated by a light-gray rectangle that encompasses the Stansbury event. The youngest sub-Provo date occurs after the Stansbury event, reflecting probable contamination with modern carbon.

Much of the BL04-4 $\delta^{18}O$ record resembles the GISP2 $\delta^{18}O$ record, suggesting the possibility that DO-scale variability in North Atlantic temperatures and eastern Great Basin precipitation were linked; i.e., 11 DO events occur are associated with relatively wet periods in the Bonneville Basin. The three lake-size proxy records (Fig. 8B–D) indicate that H2, H3, and H4 occurred during periods of relative aridity, and H2 appears to occur during the last of the Stansbury Oscillations. It is not clear whether H1 is associated with a relatively dry period, because H1 occurs during the Provo event, and relative spill rates over that time period are unknown. However, at 15.9 ka low-mg calcite precipitation ceases, TIC precipitation increases, and $\delta^{18}O$ values sharply increase (Fig. 2), suggesting a brief oscillation of lake level beneath the Provo at nearly the same time as H1 (15.8 ka). Heinrich events were associated with wet–dry transitions in BL04-4, suggesting that either the warming associated with the recovery from a Heinrich event increased the evaporation rate of Lake Bonneville and (or) that the core of the polar jet stream (PJS) shifted north of the Bonneville Basin in response to Heinrich events.

Even though the BL04-4 $\delta^{18}O$ record is noisier than the GISP2 $\delta^{18}O$ record, the early part of the BL04-4 $\delta^{18}O$ record (43–37 ka) resembles the GISP2 $\delta^{18}O$ record in that four Bonneville $\delta^{18}O$ minima can be correlated to four GISP2 $\delta^{18}O$ maxima (Fig. 8A, D), and, arguably, the two records can also be correlated between 37 and 27 ka. In addition, the overall cold condition that existed between H2 and H1 in the North Atlantic is associated with a wet oscillation in the BL04-4 records.

There is little correlation between the GISP2 $\delta^{18}O$ record between 21 and 15 ka. This was the time when the Laurentide Ice Sheet was large and when the Bonneville Basin was very wet. However, there appears to be no relation between GISP2 air temperature variability and Great Basin wetness, probably because GISP2 air temperatures were not reflecting changes in ice volume or North Atlantic circulation patterns as temperature did during previous H and DO events.

The fall of Lake Bonneville from the Provo level occurred during the Oldest Dryas interval and the fall of Lake Bonneville from the Gilbert level occurred at the termination of the Younger Dryas interval. The low lake interval that follows the Gilbert event is associated with the Pre-Boreal Oscillation (PBO). Thus, many oscillations in the hydrologic balance of Lake Bonneville appear related to oscillations in North Atlantic air temperature.

5.6. Change in LIS shape during Heinrich events and their effect on Bonneville lake levels

Dyke et al. (2002) have suggested that H1 "probably drew down the entire central ice surface" which was positioned over Hudson Bay. Such a change in topography should have affected the wind-field, including the trajectory of the PJS, in agreement with the hypothesis of Wunsch (2006). Recent estimates of sea-level change during H4 (Chappell, 2002; Roche et al., 2004) yield some insight into how much ice is lost from the LIS during a Heinrich event; unfortunately, the studies yielded very different estimates of sea-level change and the absolute increase in sea level due to a Heinrich

event remains a subject of debate. Chappell (2002) calculated that 10–15 m increases in sea level occurred during H4. Clark et al. (2007) recently modeled the response of sea level to changes in the mass balance of Northern Hemisphere ice sheets forced by variable Atlantic and Pacific sea-surface temperatures. These simulations, which indicate that H4 was accompanied by 17 m of sea-level rise, support the work of Chappell (2002).

Bintanja et al. (2005) has calculated the amount of water stored in the LIS during the past 1.2 Ma. The amount of water stored in the LIS just prior to H1, H2, and H4 and estimates of sea level change, ranging from 2 to 15 m, were used to calculate the percentage of LIS ice transported to the North Atlantic during a Heinrich event, assuming all the ice came from the LIS. The calculations indicate values ranging from 3 to 38% of the total mass of the LIS (Table 3). Accepting the calculations of Chappell (2002) and Clark et al. (2007), a large percentage of the LIS appears to have been lost to the North Atlantic during Heinrich events and the resulting change in the size and shape of the LIS may have influenced the positioning of the PJS over the western United States.

5.7. Late Wisconsin glaciations of the Uinta and Wasatch mountains and their relation to Bonneville lake levels

Well-constrained cosmogenic surface-exposure Beryllium-10 (^{10}Be) ages for two Last Glacial Maximum (LGM) moraines (Lake Fork 1, Lake Fork 2) in the southwestern Uinta Mountains have ranges, respectively, of 17.1 ± 1.5–19.9 ± 2.0 ka and 16.5 ± 1.5–18.4 ± 1.9 ka and means, respectively, of 18.4 ± 1.1 ka and 17.2 ± 0.7 ka (Munroe et al., 2006). All ^{10}Be ages used in this paper have been calculated using a production rate of 4.98 atoms g SiO_2/yr and have been labeled ka.

Munroe et al. (2006) used this data to suggest that deglaciation of the southwestern Uinta Mountains began at 17.2 ± 0.7 ka. In the western Uinta Mountains, surface-exposure (^{10}Be) ages for two moraines (Manor Lands, Proximal Ridge) yield ranges, respectively, of 16.3 ± 1.8–18.5 ± 2.2 ka and 17.1 ± 1.6–19.2 ± 1.7 ka and means, respectively, of 17.1 ± 0.7 ka and 18.5 ± 0.7 ka (Laabs et al., 2007), also suggesting the beginning of glacial contraction at ~17 ka.

Elevated values of hard isothermal remanent magnetization (HIRM) from Bear Lake, Utah (which drained the western Uinta ice field), have been interpreted to indicate glacial activity in the Uinta Mountains between 32 and ≤17 ka, with the maximum extent of the Bear River glacier occurring at 25 ka (Rosenbaum, 2005). Laabs et al. (2007) suggest that the cosmogenic surface-exposure ages of the two western Uinta moraines and the glacial-proxy data from Bear Lake together indicate that the glaciation of the western Uintas remained at a near-maximum state between 25 and ~18.7/18.1 ka.

Cosmogenic ^{10}Be surface-exposure ages of moraines deposited after the Bonneville flood, downvalley from the mouths of Little Cottonwood and Bells canyons on the western flank of the Wasatch, have ages ranging from 16.9 ± 0.4 to 15.2 ± 0.4 ka with a mean age of 15.9 ± 0.7 ka (Lips et al., 2005). Lips (personal communication, 2007) has suggested that the relatively young ages of these moraines are due to lake-effect precipitation generated by Lake Bonneville. During storms, the Wasatch Mountains acted as an

Table 3
Percent reduction in size of Laurentide Ice Sheet.

Heinrich event	Increase in sea level			
	2 m	5 m	10 m	15 m
H1	3.1	7.7	15.4	23.1
H2	3.3	8.3	16.7	25.0
H3	4.0	10.0	20.0	30.0
H4	5.0	12.5	25.0	37.5

Table 4
Timing of Lake Bonneville hydrologic events.

Lake Bonneville Hydrologic Event	Blue Lake Core BL04-4	Outcrop-Based Lake-Level Record
	PSV-Based age model (ka)	0 ka Reservoir effect (ka)
Stansbury Oscillation(s)	26.0–23.0	25.8–24.3
Initiation of Lake Bonneville overflow	18.5	≤18.6
Fall from the Bonneville highstand	17.0	17.5
Beginning of the Provo event	17.0	17.4
Fall from Provo level	15.2	13.8 (Godsey)[a] or 17.0 (Oviatt)[b]
Gilbert event	13.1–11.6	12.9–11.2

[a] Godsey refers to Godsey et al. (2005).
[b] Oviatt refers to Oviatt (1997).

orographic barrier, preventing buildup of snow and ice in the Uinta Mountains which lie downwind of the Wasatch; hence, the Uintas failed to produce the last phase of alpine glaciation that occurred in the Wasatch Mountains.

The growth of the western Uinta Mountain glaciers paralleled the growth of Lake Bonneville between 32 and 24 ka; i.e., proxy lake-size records (e.g., TIC and $\delta^{18}O$) level off at times when the glaciers oscillated about their maximum downvalley positions (Fig. 8). The Uinta and western Uinta Mountain glaciers began to recede at about the time Lake Bonneville fell to the Provo level (∼17 ka) and the Wasatch Mountain glaciers achieved their maximum extent by the end of the Provo event (15.2 ka) (Fig. 8). Given that alpine glacial extent is correlated with lake surface area, the size of the alpine glaciers was, to a large extent, governed by "lake-effect" moisture. This concept is consistent with the modeling results of Hostetler and Giorgi (1992) and Hostetler et al. (1994).

6. Summary and conclusions

High-resolution records of lake-size variability presented in this paper are in general but not specific agreement with the Lake Bonneville time-elevation envelope developed by Oviatt et al. (1992) (Fig. 2A) (Table 4). The lake-level envelope has the advantage of providing a measure of minimum lake elevation over time whereas the Blue Lake core climate-proxy records have the advantage of providing nearly continuous to continuous records of relative lake-size change. The carbon-based parts of the lake-level envelope have issues when it comes to reservoir effect; in addition, some of the carbonate samples used to create the lake-level record may have become contaminated with modern carbon during subaerial exposure. The sediment-based records of change in hydrologic balance sometimes include sporadic inputs of older reworked sediment whose isotopic, mineralogical, and chemical signatures dilute the autochthonous record.

The BL04-4 $\delta^{18}O$ and TIC records clearly show the Stansbury Oscillation as a pair of oscillations (Fig. 2D, E). In the climate-proxy records, H2 occurs during the last Stansbury Oscillation (Fig. 8C, D). The Bonneville highstand is represented by the decreases in $\delta^{18}O$ and TIC that began at 18.5 ka (Fig. 2B, D). Incision of the Bonneville Basin began at 17.0 ka and Lake Bonneville occupied the Provo level between 17.0 and 15.2 ka, with the fall from the Provo level occurring between 15.2 and 14.7 ka during the Oldest Dryas interval. In addition, the Gilbert wet event appears to coincide with the Younger Dryas cold interval (12.9–11.6 ka).

The apparent connection between Greenland air temperatures and eastern Great Basin wetness appears to change over time.

Between 45 and 15 ka, wet events in the Bonneville Basin are associated with warm events in the North Atlantic; and relatively dry periods in the Bonneville Basin are associated with cold events in the North Atlantic however, after 15 ka, the Gilbert wet event in the Bonneville Basin was associated with a North Atlantic cold interval − the Younger Dryas event.

Sediment from the Bear River glacier in the western Uinta Mountains reached Bear Lake ∼32 ka, indicating the onset of glaciation. This glacier advanced until 24 ka when it reached its maximum extent. Surface-exposure ages of boulders deposited by the Bear River glacier and boulders deposited by glaciers in the southwestern Uinta Mountains indicate that glacial retreat could have begun as late as 17 ka (Munroe et al., 2006; Laabs et al., 2007). Of particular interest is the fact that the growth of the Bear River glacier between 32 and 17 ka paralleled changes in the values of proxy indicators of Bonneville Basin wetness (Fig. 8) and that terminal moraines on the western side of the Wasatch Mountains have ages ranging from 16.9 to 15.2 ka. This suggests a near synchroneity of change in the hydrologic and cryologic balances occurring in the Bonneville drainage system and that glacial extent was linked to lake size. This reinforces suggestions by Munroe et al. (2006) and Laabs et al. (2007) that Lake Bonneville acted as a moisture source for glaciers in the downwind mountains.

Appendix. Supplementary data

Supplementary data related to this article can be found online at doi:10.1016/j.quaint.2010.12.014.

References

Antevs, E., 1948. Climatic changes and pre-white man. In: The Great Basin, with Emphasis on Glacial and Post-Glacial Times, vol. 38. University of Utah, pp. 168–191. Bulletin.
Benson, L.V., Thompson, R.S., 1987. The physical record of lakes in the Great Basin. In: Ruddiman, W.F., Wright Jr., H.E. (Eds.), North America and Adjacent Oceans during the Last Deglaciation. The Geology of North America V. K-3. The Geological Society of America, Boulder.
Benson, L., Paillet, F., 2002. HIBAL: a hydrologic-isotopic-balance model for application to paleolake systems. Quaternary Science Reviews 21, 1521–1539.
Benson, L.V., Lund, S.P., Burdett, J.W., Kashgarian, M., Rose, T., Smoot, J.P., Schwartz, M., 1998. Correlation of late Pleistocene lake-level oscillations in Mono Lake, California, with North Atlantic climate events. Quaternary Research 49, 1–10.
Benson, L., Kashgarian, M., Rye, R., Lund, S., Paillet, F., Smoot, J., Kester, C., Mensing, S., Meko, D., Lindstrom, S., 2002. Holocene multidecadal and multicentennial droughts affecting Northern California and Nevada. Quaternary Science Reviews 21, 659–682.
Bintanja, R., van de Wal, R.S.W., Oerlemans, J., 2005. Modelled atmospheric temperatures and global sea levels over the past million years. Nature 437, 125–128.
Bond, G., Broecker, W., Johnsen, S., McManus, J., Labeyrie, L., Jouzel, J., Bonani, G., 1993. Correlations between climate records from North Atlantic sediments and Greenland ice. Nature 365, 143–147.
Bright, 1966. Pollen and seed stratigraphy of Swan Lake, southeastern Idaho: its relation to regional vegetation history and to Lake Bonneville history. Tebiwa 9, 1–28.
Chappell, J., 2002. Sea level changes forced ice breakouts in the Last Glacial cycle; new results from coral terraces. Quaternary Science Reviews 21, 1229–1240.
Clark, P.U., Hostetler, S.W., Pisias, N.G., Schmittner, A., Meissner, K.J., 2007. Mechanisms for a ∼7-kyr climate and sea-level oscillation during Marine Isotope Stage 3. In: Schmittner, A., Chiang, J., Hemming, S. (Eds.), Ocean Circulation: Mechanisms and Impacts Past and Future Changes of Meridional Overturning, vol. 173. American Geophysical Monograph, pp. 209–246.
Currey, D.R., Oviatt, C.G., 1985. Durations, average rates, and probable causes of Lake Bonneville expansions, stillstands, and contractions during the last deep-lake cycle 32,000 to 10,000 years ago. Geographical Journal of Korea 10, 1085–1099.
Dansgaard, W., Johnsen, S., Clausen, H.B., Dahl-Jensen, E., Gudnestrup, N.S., Hammer, C.U., Hvidberg, C.S., Steffensen, J.P., Sveinbjornsdottir, A.E., Jouzel, J., Bond, G., 1993. Evidence for general instability of past climate from a 250-kyr ice-core record. Nature 364, 218–220.
Dyke, A.S., Andrews, J.T., Clark, P.U., England, J.H., Miller, G.H., Shaw, J., Veillette, J., 2002. The Laurentide and innuitian ice sheets during the last glacial maximum. Quaternary Science Reviews 21, 9–32.
Gilbert, G.K., 1890. Geological Survey Monograph, Lake Bonneville. U.S., p. 1,438.
Godsey, H.S., Currey, D.R., Chan, M.A., 2005. New evidence for an extended occupation of the Provo shoreline and implications for regional climate change, Pleistocene Lake Bonneville, Utah, USA. Quaternary Research 63, 212–223.

Hart, W.S., Madsen, D.B., Kaufman, D.S., Oviatt, C.G., 2004. The $^{87}Sr/^{86}Sr$ ratios of lacustrine carbonates and lake-level history of the Bonneville paleolake system. Geological Society of America Bulletin 116, 1107–1119.

Hostetler, S.W., Benson, L.V., 1990. Paleoclimatic implications of the high stand of Lake Lahontan derived from models of evaporation and lake level. Climate Dynamics 4, 207–217.

Hostetler, S.W., Giorgi, F., 1992. Use of a regional atmospheric model to simulate lake–atmosphere feedbacks associated with Pleistocene Lakes Lahontan and Bonneville. Climate Dynamics 7, 39–44.

Hostetler, S.W., Giorgi, F., Bates, G.T., Bartlein, P.J., 1994. Lake–atmosphere feedbacks associated with paleolakes Bonneville and Lahontan. Science 263, 665–668.

Johnson, T.C., Lynch, E.L., Showers, W.J., Palczuk, N.C., 1988. Pleistocene fluctuations in the western boundary undercurrent on the Blake Outer Ridge. Paleoceanography 3, 191–207.

Keigwin, L.D., Jones, G.A., 1994. Western North Atlantic evidence for millennial-scale changes in ocean circulation and climate. Journal of Geophysical Research 99, 12,397–12,410.

Kutzbach, J.E., Guetter, P.J., 1986. The influence of changing orbital parameters and surface boundary conditions on climate simulations for the past 18,000 years. Journal of Atmospheric Science 43, 1726–1759.

Laabs, B.J.C., Munroe, J.S., Rosenbaum, J.G., Refsnider, K.A., Mickelson, D.M., Singer, B.S., Caffee, M.W., 2007. Chronology of the last glacial maximum in the upper Bear River basin, Utah. Arctic, Antarctic, and Alpine Research 39, 537–548.

Light, A., 1996. Amino acid paleotemperature reconstruction and radiocarbon shoreline chronology of the Lake Bonneville Basin, USA, University of Colorado, M.Sc. thesis.

Lips, E.W., Marchetti, D.W., Gosse, J.C., 2005. Revised Chronology of Late Pleistocene Glaciers, Wasatch Mountains, Utah, vol. 37. Geological Society of America. Abstracts with Programsp. 41.

Louderback, L.A., Rhode, D.E., 2009. 15,000 years of vegetation change in the Bonneville basin: the Blue Lake pollen record. Quaternary Science Reviews 28, 308–326.

Lund, S.P., 1996. A comparison of Holocene paleomagnetic secular variation records from North America. Journal of Geophysical Research 101, 8007–8024.

Lund, S.P., Keigwin, L., 1994. Measurement of the degree of smoothing in sediment paleomagnetic secular variation records: an example from late Quaternary deep-sea sediments of the Bermuda Rise, western North Atlantic Ocean. Earth and Planetary Science Letters 122, 317–330.

Lund, S.P., Schwartz, M., Keigwin, L., Johnson, T., 2005. Deep-sea sediment records of the Laschamp geomagnetic field excursion (~41,000 cal. yrs. BP). Journal of Geophysical Research 110, B04101.

Lund, S.P., Liddicoat, J.C., Lajoie, K.L., Henyey, T.L., Robinson, S.W., 1988. Paleomagnetic evidence for long-term (10^4 year) memory and periodic behavior in the Earth's core dynamo process. Geophysical Research Letters 15, 1101–1104.

Lund, S.P., Williams, T., Acton, G., Clement, B., Okada, M., 2001a. Brunhes Epoch magnetic field excursions recorded in ODP Leg 172 sediments. In: Keigwin, L., Rio, D., Acton, G. (Eds.) Proceedings of the Ocean Drilling Project, Scientific Results vol. 172, Ch. 10.

Lund, S.P., Acton, G., Clement, B., Okada, M., Williams, T., 2001b. Paleomagnetic records of Stage 3 excursions from ODP Leg 172 sediments. In: Keigwin, L., Rio, D., Acton, G. (Eds.) Proceedings of the Ocean Drilling Project, Scientific Results vol. 172, Ch. 11.

Malde, H.E., 1968. Idaho. U.S. Geological Survey Professional Paper. The Catastrophic Late Pleistocene Bonneville Flood in the Snake River Plain, vol. 596 p. 52.

Munroe, J.S., Laabs, B.J.C., Shakun, J.D., Singer, B.S., Mickelson, D.M., Refsnider, K.A., Caffee, M.W., 2006. Latest Pleistocene advance of alpine glaciers in the southwestern Uinta Mountains, Utah, USA: evidence for the influence of local moisture sources. Geology 34, 841–844.

Oviatt, C.G., 1991. Quaternary Geology of the Black Rock Desert, Millard County, Utah Special Studies-Utah Geological and Mineralogical Survey 73.

Oviatt, C.G., 1997. Lake Bonneville fluctuations and global climate change. Geology 25, 155–158.

Oviatt, C.G., Currey, D.R., Sack, D., 1992. Radiocarbon chronology of Lake Bonneville, Eastern Great Basin, USA. Palaeogeography, Palaeoclimatology, Palaeoecology 99, 225–241.

Oviatt, C.G., Miller, D.M., McGeehin, J.P., Zachary, C., Mahan, S., 2005. The younger Dryas phase of great salt Lake, Utah, USA. Palaeogeography, Palaeoclimatology, Palaeoecology 219, 263–284.

Roche, D., Paillard, D., Cortijo, E., 2004. Duration and iceberg volume of Heinrich event 4 from isotope modelling study. Nature 432, 379–382.

Rosenbaum, J. G., 2005. Magnetic properties of sediments in cores BL-1, -2 and -3 from Bear Lake, Utah and Idaho. U. S. Geological Survey Open-File Report 2005-1203, p. 30.

Russell, I.C., 1885. Geological History of Lake Lahontan, A Quaternary Lake of Northwestern Nevada, vol. 11. U.S. Geological Survey Monograph.

Sack, D., 1999. The composite nature of the Provo level of Lake Bonneville, Great Basin, western North America. Quaternary Research 52, 316–327.

Spencer, R.J., Baedecker, M.J., Eugster, H.P., Forester, R.M., Galdhaber, M.B., Jones, B.F., Kelts, K., McKenzie, J., Madsen, D.B., Rettig, S.L., Rubin, M., Bowser, C.J., 1984. Great Salt Lake, and precursors, Utah: the last 30,000 years. Contributions to Mineralogy and Petrology 86, 321–334.

Stanley, S.M., Ries, J.B., Hardie, L.A., 2002. Low-magnesium calcite produced by coralline algae in seawater of Late Cretaceous composition. Proceedings of the National Academy of Sciences 99, 15323–15326.

Stuiver, M., Grootes, P.M., Braziunas, 1995. The GISP2 $\delta^{18}O$ climate record of the past 16,500 years and the role of the sun, ocean, and volcanoes. Quaternary Research 44, 341–354.

Stuiver, M., Reimer, P.J., Reimer, R.W., 2005. CALIB 5.0 [WWW program and documentation].

Wunsch, C., 2006. Abrupt climate change: an alternative view. Quaternary Research 65, 191–203.